HHS Public Access

Author manuscript

Laryngoscope. Author manuscript; available in PMC 2019 March 01.

Published in final edited form as:

Laryngoscope. 2018 March ; 128(3): E105–E110. doi:10.1002/lary.26962.

In vivo Imaging of the Internal Nasal Valve during different conditions using Optical Coherence Tomography

Anna S. Englhard, MD[1], **Maximilian Wiedmann, MS**[3], **Georg J. Ledderose, MD**[1], **Bryan Lemieux, MD**[2], **Alan Badran, BS**[2], **Joseph C. Jing, PhD**[3], **Zhongping Chen, PhD**[3], **Veronika Volgger, MD**[1], and **Brian J. F. Wong, MD, PhD**[2,4]

[1]Department of Otolaryngology - Head and Neck Surgery, Ludwig Maximilian University Munich, 81733 Munich, Germany

[2]Beckman Laser Institute, University of California Irvine, Irvine, CA 92612, USA

[3]Department of Biomedical Engineering, University of California Irvine, Irvine, CA 92612, USA

[4]Department of Otolaryngology - Head and Neck Surgery, University of California Irvine, Orange, CA 92868, USA

Abstract

Objective—Previously, we proposed long-range optical coherence tomography (LR-OCT) to be an effective method for the quantitative evaluation of the nasal valve geometry. Here, the objective was to quantify the reduction in the internal nasal valve angle and cross-sectional area that results in subjective nasal airway obstruction and to evaluate the dynamic behavior of the valve during respiration using LR-OCT.

Methods—For 16 healthy individuals, LR-OCT was performed in each naris during: 1) normal respiration; 2) peak forced inspiration; 3) lateral nasal wall depression (to the onset of obstructive symptoms); and 4) after application of a topical decongestant. The angle and the cross-sectional area of the valve were measured.

Results—A reduction of the valve angle from 18.3° to 14.1° (11° in Caucasians and 17° in Asians) and a decrease of the cross-sectional area from 0.65 cm^2 to 0.55 cm^2 led to subjective nasal obstruction. Forceful breathing did not significantly change the internal nasal valve area in healthy individuals. Application of nasal decongestant resulted in increased values.

Conclusion—LR-OCT proved to be a fast and readily performed method for the evaluation of the dynamic behavior of the nasal valve. The values of the angle and the cross-sectional area of the valve were reproducible and changes in size could be accurately delineated.

Correspondence: Brian J. Wong, Department of Otolaryngology, - Head and Neck Surgery, University of California Irvine, Orange, CA 92868, USA, Tel.: 714-456-7017, bjwong@uci.edu.

First results of the study were presented at the 86th Annual Meeting of the German Society of Oto-Rhino-Laryngology, Head and Neck Surgery in Berlin, Germany, May 14th-16th, 2015 and at the 7th Scientific Meeting of the Head and Neck Optical Diagnostics and Intervention Society in London, England, July 24th, 2015.

The authors have no funding, financial relationships, or conflicts of interest to disclose.

Keywords

optical coherence tomography; internal nasal valve; nasal obstruction; endoscopy; long-range Fourier-domain

Introduction

Nasal airway obstruction and the commonly associated reduced quality of life metrics are one of the most common complaints of patients, and the cost of medical therapy and surgical treatment of this symptom is immense.[1-4] For example, over 250,000 septoplasty operations are performed each year to treat airway obstruction.[5] Although symptoms of nasal obstruction can have several etiologies, such as mucosal congestion, septal deviation, and others, incompetence of the internal nasal valve is a common cause, and often missed as a diagnosis even by experts.[6-8] It is estimated that about 13 % of the general and up to 60 % of the geriatric population in the US have some form of internal nasal valve malfunction.[9,10]

The internal nasal valve (INV) is the narrowest part of the nasal airway and therefore the site of maximum resistance.[6] It is limited laterally by the upper lateral cartilages, inferiorly by the anterior end of the inferior turbinate and medially by the septum.[8] A purported angle of about 10 - 15° exists between the upper lateral cartilage and the septum in patients without nasal obstruction[7,11,12], below which the valve is considered to be at risk for dynamic collapse;[7] however, an exact value or range of values has not been rigorously identified, and the geometry is much more complex than a simple solid angle.[13] Minor changes in the geometry of the nasal valve region may have a significant impact on airflow, which in turn affects nasal function and the perception of airway patency. As a result, improving or correcting flow through the nasal valve region is an active area of interest for surgeons who perform functional rhinoplasty, an operation that is part of the surgical armamentarium used to treat sleep disordered breathing.

Existing tools, including rhinomanometry, acoustic rhinometry[14-16] or computed tomography[17-20], have been proposed as means to directly or indirectly gauge flow, nasal airway resistance, and internal nasal valve area; however, each of these diagnostic tests have limitations[6,8,21,22]. Thus, there is no objective measure to determine internal nasal valve obstruction, and surgeons rely upon the physical examination, nasal endoscopy, clinical judgment or patient reported outcome measures[2] to make decisions to pursue surgery and then select the appropriate airway operation that may vary from being very simple (septoplasty and turbinate reduction) to complex (functional rhinoplasty and nasal valve repair).[8,22]

Optical coherence tomography (OCT) is a novel non-invasive method for the evaluation of the INV area.[23] OCT acquires high resolution (10 μm), cross-sectional images of tissue.[24] In otorhinolaryngology, OCT has mainly been used to examine tissue structure with a focus on cancerous or dysplastic lesions. A variant of conventional OCT – long range- OCT (LR-OCT) – has recently been suggested as an optical rangefinder.[25,26] LR-OCT enables the assessment of the structural anatomy of hollow organs, such as the upper airway, and the generation of volumetric representations.[26,27] In a previous study we demonstrated that OCT

accurately quantifies internal nasal valve geometry, and the measured values for angle and cross-sectional area correlated well with nasal endoscopy.[23] While commonplace, nasal endoscopy is significantly less precise and very subjective as geometry is estimated from two-dimensional projections of a true 3 D surface.

Here we imaged the internal nasal valve using LR-OCT to quantify changes in valve angle and cross-sectional area during: 1) normal respiration; 2) peak forced inspiration; 3) lateral nasal wall depression (to the onset of obstructive symptoms); and 4) after application of a topical decongestant. Hereby, we aimed to evaluate the dynamic behavior of the INV during respiration and to quantify the reduction in valve angle and cross-sectional area that results in obstructive symptoms.

Material and Methods

Study design

This study was approved by the Institutional Review Board at the University of California Irvine. We measured the internal nasal valve under different physiological conditions using LR-OCT in 16 healthy individuals without history of nasal airway obstruction, allergies, recurrent sinusitis, or previous nasal surgery or rhinoplasty. For each subject, LR-OCT was conducted in both nasal airways. The cross-sectional area and the angle of the valve were assessed (figure 3). OCT measurement of both right and left sides were performed at rest, during vivid forced inspiration, and during the gradual application of force along the nasal sidewall using a specialized nasal device in order to identify the onset of nasal obstruction (figure 2).

All data was collected in the same patient group. In a first step the internal nasal valve angle and the cross-sectional area in normal and decongested conditions were evaluated. In a second step the values of the angle and the area during inspiration and with external pressure in normal and decongested conditions were measured for the same individuals.

LR- OCT system

For LR- OCT imaging a specially constructed swept source Fourier Domain-OCT system was used which has been previously reported and is only briefly described here.[23,26,27] OCT-measurements are 1-dimensional distances from the probe. Rotation of the probe is required in order to build a 2-dimensional cross-section of the nasal cavity. Here, for the rotational scanning of the OCT probe an external rotational motor (Animatics; Santa Clara, CA, USA) was connected to a fiber optic rotary joint (Princetel Inc.; Pennington, NJ, USA). Rotation from the motor was transmitted through the coil to the distal probe tip. A dual-motor stage (Zaber Technologies Inc.; Vancouver, BC, Canada) enabled simultaneous linear pullback of the probe towards the naris. This allowed for image acquisition in a helical, retrograde way.

OCT Imaging during Rest and Forced Inspiration

OCT imaging of the internal nasal valve was performed on seated, awake individuals bilaterally (figure 1). No local anesthetic was applied prior to inserting the OCT probe.

Probe rotation and pullback, data acquisition and real-time image display were controlled by software operating on a Windows platform. The OCT probes were coated with a transparent single use fluorinated ethylenepropylene (FEP) sheath (Zeus Inc.; Orangeburg, SC, USA). The distal end of these sheaths was treated with a butane lighter to provide a hermetic seal. The outer diameter of the probe was 1.2 mm, including sheath it measured 2.1 mm. Using a nasal speculum, the probe was introduced into the nasal cavity and advanced along the floor of the nose. The speculum was then removed. In the nasopharynx, the probe was rotated (25 Hz) and linearly retracted (3.13 mm/s) within the sheath. 500 images with 125 μm separation between consecutive frames were acquired in a spiral way. During pullback, the sheath was held stationary on the floor of the nose. Image acquisition began in the nasopharynx and ended when the probe tip was outside the nose. Subsequently, OCT imaging was repeated on both sides during forced inspiration, where the subject was asked to inspire rapidly to trigger lateral wall movement.

OCT Imaging during Nasal Sidewall Displacement

In order to measure the valve angle at the subjective onset of nasal obstruction symptoms, we developed a simple mechanical device to displace the lateral nasal wall (upper lateral cartilage). This specially designed nasal device was placed externally and unilaterally over the nasal valve area (figure 2). This device is a mounted a hardhat and consists of a cantilevered apparatus supporting a caliper. The caliper has inward facing points to which a small blunt footpad is attached. The caliper is easily adjusted to either be in non-contact, near contact, or in contact with the lateral sidewall of the nose at the level of the distal upper lateral cartilage. Adjustment of a setscrew on the caliper allows gentle displacement of the sidewall while displacement is monitored on a digital readout. Patients were asked to breathe normally while the caliper displacement was slowly increased until the onset of subjective nasal obstruction was reached. The value of the digital readout was noted. This procedure was repeated three times and the mean for the three time points was calculated. The process was repeated on the opposite side. OCT imaging was performed at the onset of subjective nasal obstruction as defined above with the caliper placed over the nasal valve area.

OCT Imaging during Decongestant Application

Subsequently, decongestant nasal spray (oxymetazoline hydrochloride, 0.05%, taro pharmaceuticals, Hawthorne, NY USA) was sprayed once in the nasal vault; after five minutes elapsed OCT imaging was repeated for both sides with and without the nasal device and during forced inspiration. The time to acquire one set of OCT images was approximately one minute. Overall procedural time including equipment setup and data acquisition was about twenty minutes for all circumstances as noted above.

Data Analysis

Continuous helical scanning from the nasopharynx to the naris produced about 500 raw images for each OCT data set. These images were post-processed to BMP file format (2000 × 2048 pixels). The offline data analysis included a frame-by-frame examination of the OCT data within a graphic viewer (IrfanView; Irfan Skiljan, Austria). For the identification of the airway anatomy, the OCT data were transformed from Cartesian to polar coordinates in MatLab. This rendered the data into an anatomic (axial) configuration and facilitated both

visualization and analysis. The INV was identified by the septum and the anterior head of the inferior turbinate (figure 3).[8] Seven separate serial images just posterior of the beginning of the inferior turbinate were selected and loaded into Photoshop CC (Adobe systems, San José, CA, USA). Calculations were performed on all seven images and the mean was calculated. Measurements included the angle and the cross-sectional area of the internal nasal valve (figure 4). The nasal valve angle was measured along the medial and lateral borders of the airway lumen visually averaging the contour irregularities. The area was obtained along the margins of the airway lumen. For this, the sheath diameter was used as a scale. The cross sectional area was then calculated by counting the number of pixels inside of the sheath using ImageJ.

For multiple group comparisons the Kruskal-Wallis test followed by Dunn's test were applied. Differences were considered statistically significant at $p<0.05$.

Results

LR-OCT was performed in 32 nasal vaults of 16 healthy subjects. Six patients were female and ten were male. Eight (three female and five male) individuals were Caucasian and eight (three female and five male) were Caucasian. All 32 cases were completed, without the occurrence of any adverse events.

All 32 data sets demonstrated the gross contour of the nasal airway. The anterior head of the inferior turbinate and the septum were easily identified in each subject.

Internal nasal valve angle

The INV angle was 18.3° ± 3.1° (mean ± SD). During forced inspiration the mean angle was found to be 17.3° ± 6.1° (mean ± SD), which was not a statistically significant difference (figure 4 and 5). When the upper lateral cartilage was displaced by the device to the point of symptom onset, INV was found to be smaller at 14.1° ± 5.9° (mean ± SD) ($p<0.05$). After application of nasal decongestant the internal nasal valve angles were 21.7° ± 5.9° (mean ± SD); this increase was statistically significant compared to the angle in normal conditions ($p < 0.05$). During forced inspiration after application of decongestant the angle was 21.2° ± 6.4° (mean ± SD), which was not statistically significant when compared to the values after application of nasal decongestant alone (figure 5). With external pressure on the nasal valve area after application of nasal decongestant the angle was statistically significantly smaller than with decongestant alone (18.7° ± 5.1° (mean ± SD)) ($p<0.05$).

Cross-sectional area

The cross-sectional area measured by OCT was 0.65 cm^2 ± 0.23 cm^2 (mean ± SD) and did not change statistically during forced inspiration (0.63 cm^2 ± 0.25 cm^2 (mean ± SD) ($p<0.05$). With external pressure on the nasal valve area, the area was statistically smaller (0.55 cm^2 ± 0.23 cm^2 (mean ± SD)) ($p<0.05$). After application of nasal decongestant the cross-sectional area was found to be 0.97 cm^2 ± 0.31 cm^2 (mean ± SD), which was statistically larger compared to the INV under normal conditions ($p < 0.05$) (figure 5). During forced inspiration after application of nasal decongestant the cross-sectional area was not significantly changed compared to conditions with nasal decongestant alone (0.97 cm^2

± 0.27 cm^2 (mean ± SD)). With external pressure on the nasal valve area after application of nasal decongestant the cross-sectional area was not statistically significantly changed when compared to conditions with nasal decongestant alone (0.95 cm^2 ± 0.29 cm^2 (mean ± SD)) (figure 6).

Subpopulation

As in our previous works, we opted to perform a subgroup analysis based on purported anatomic variances that exist between Asians and Caucasians. In the Asian subpopulation the INV angle was found to be 21.7° ± 3.0° (mean ± SD), and the area measured 0.65 cm^2 ± 0.21 cm^2 (mean ± SD). With external pressure on the nasal valve area both the INV angle and the cross-sectional area were statistically significantly smaller (17.4° ± 6.0° (mean ± SD)) ($p<0.05$) and 0.56 cm^2 ± 0.24 cm^2 (mean ± SD)) ($p<0.05$). In the Caucasian subpopulation the INV angle was found to be 14.2° ± 3.2° (mean ± SD), the cross-sectional area measured 0.65 cm^2 ± 0.23 cm^2 (mean ± SD). With external pressure on the nasal valve area both the INV angle and the cross-sectional area were statistically significantly smaller (11.0° ± 5.8° (mean ± SD)) ($p<0.05$) and (0.55 cm^2 ± 0.22 cm^2 (mean ± SD)) ($p<0.05$).

Discussion

Internal nasal valve incompetence, insufficiency, or collapse is a major cause of nasal obstruction, and a component of sleep disordered breathing.[6-8] The indications for nasal valve surgery have recently been defined and clinical practice guidelines for functional rhinoplasty have been described.[28] Textbooks state that symptomatic nasal valve collapse occurs when INV angle is less than 10 – 15°, although the value of a single angle or measurement remains heavily debated.[7,11,12,29] It is well known that even minor changes of the nasal valve region may have significant impact on nasal airflow,[30] however, it is unclear, what degree of reduction in the INV angle leads to subjective nasal obstruction. Previously, we proposed LR-OCT to be an effective method for the quantitative evaluation of the nasal valve geometry, as its' resolution is over two orders of magnitude greater than either CT or MRI imaging.[23] LR-OCT is relatively fast and easily performed, and accurately quantifies the INV area as well as geometry. The values of the angle and the cross sectional area of the internal nasal valve were reproducible and correlated well to the data seen with endoscopy.[23] Endoscopy is challenging to employ, as fish eye optics of nasal endoscopes plus estimation of angle from 2D images of a 3D surface that varies in depth makes consistent examination vary from user to user. As such, nasal endoscopy is not universally accepted as the mainstay for diagnosing INV insufficiency.[8]

Here, LR-OCT again demonstrated speed and ease of use as a method for objective evaluation of the INV. It was safe and well tolerated in patients without the need for sedation or local anesthesia. A reduction of the INV angle by 4.2° to a value of 14.1° measured by OCT correlated with the subjective onset of nasal airway obstruction. This angle of 14.1° is slightly larger than the classically described definition of an INV collapse below 10 – 15°.[7,11,12]

However, these values were collected from a Caucasian population, whereas only 50% of our study group was Caucasian. With a mean value of 11° for the subjective beginning of

nasal airway obstruction in the Caucasian study subpopulation, the angle measured by OCT correlated well with the historical range. Previous reports show that the INV angle in Asians with values around 22° is significantly larger.[20] In our study an angle of 17.4° led to subjective beginning of nasal airway obstruction in the Asian subpopulation.

The cross-sectional area was also found to be significantly reduced by 0.08 cm^2 at the subjective beginning of nasal airway obstruction (from 0.65 cm^2 during normal conditions to 0.55 cm^2 with nasal obstruction) in the Asian and the Caucasian subpopulation, correlating well with values estimated using acoustic rhinometry[14,16] or CT scans[17,18]. Grymer[14] proposed acoustic rhinometry to evaluate the cross-sectional area of the INV before and after reduction rhinoplasty, showing that values of 0.5 cm^2 or below are predictable of nasal obstruction. Roithmann et al.[16] were able to demonstrate that patients with nasal obstruction, due to structural deformities or mucosal abnormalities, had cross-sectional areas below 0.45 cm^2. In CT scans a valve area blow 0.38 cm^2 was suggestive for clinical nasal obstruction.[18] These results could potentially signify that the reduction of the INV cross-sectional area is a better predictor of nasal airway obstruction than the decrease of the INV angle alone. The results of other studies suggest that the shape of the INV area might be more important for nasal airway obstruction than the value of the INV angle alone.[13,17]

The dynamic behavior of the INV could be reliably delineated using LR-OCT: analogous to previous studies, LR-OCT here demonstrated a significantly increased valve angle and cross sectional area after the application of nasal decongestant.[14,16,31,32] Obviously, some part of INV obstruction is due to the engorgement of inferior turbinate mucosa.[31,33,34] This effect may also be modified by decongestion of the nasal septum or swell body, which may also impact the size and shape of the INV.

Forced inspiration surprisingly did not lead to a significant reduction of the INV angle in healthy subjects without any history of nasal obstruction. A possible explanation might be the duration of the OCT examination of the nasal cavity of about 20 seconds. Most individuals were unable to inspire for this time. It is possible that the scenario at the nasal valve area may not correspond to inspiration, but to several breathing cycles or bated breath. However; other authors[4,6,35-37] described similar findings: Goode et al.[37] state that deep nasal breathing leads only to a slight collapse of the nasal valve area in healthy individuals. Fattahi[6] observed dynamic obstruction or collapse of the INV area during forceful inspiration in patients with weak upper or lower lateral cartilages but not in healthy individuals.

Because of the variability in INV configuration, an objective and reliable test of valve collapse would be of great value for both surgeons and patients. Existing tools, including classic rhinomanometry, acoustic rhinometry or computed tomography, have several limitations.[1,6,21,22] LR-OCT has the capability to accurately delineate the cross-sectional area of hollow organs, and does not create artifacts in shape as with cannulation methods that will alter the fluid dynamics. For this reason it appears to be a highly suitable method for the evaluation of the INV area.

The present study has several limitations, which should be discussed. One minor limitations of the present technique is that valve angle and the cross-sectional area is determined by following OCT derived airway contours, and there is always a subjective element in drawing tangent lines to the septum and nasal sidewalls. Mucous blocks “line of site” imaging with a drop off in signal intensity can profoundly reduce image quality.[38] Second, our sample size is relatively small. Moreover, the presented OCT-system was purpose built, and is therefore comparatively expensive. Because of the size of the nasal vault and upper airway, up to now, no commercial available OCT system (e.g., cardiovascular) can be used for this application, as they are not designed for long-range imaging. For now, OCT remains an investigational technology used to generate accurate airway models and define airway geometry *in vivo*, though this can change as the same base technology is being developed for coronary vasculature imaging.

Future planned studies by our group will focus on the correlation of the LR-OCT findings with patient symptomatology, disease-specific quality-of-life scores and clinical examination. Longitudinal studies could be done in which LR-OCT would be used as the primary tool to identify patients with nasal airway obstruction caused by collapse or obstruction of the internal nasal valve. Furthermore, LR-OCT could be useful for the evaluation of the impact of various nasal valve operations - such as batten and spreader grafts – to reduce lateral wall collapse, and increase airway geometry and flow.

In the future, we believe that LR-OCT will be a valuable method to assess the nasal valve objectively and to provide precise and valuable anatomical information regarding nasal obstruction and the impact of surgery on correcting this issue.

Acknowledgments

This research was supported by the National Institutes of Health (1R01HL103764-01 and R01 HL105215-01).

References

1. Fischer H, Gubisch W. Nasal valves--importance and surgical procedures. Facial plastic surgery : FPS. 2006; 22:266–280. [PubMed: 17131269]
2. Stewart MG, Witsell DL, Smith TL, Weaver EM, Yueh B, Hannley MT. Development and validation of the Nasal Obstruction Symptom Evaluation (NOSE) scale. Otolaryngology--head and neck surgery : official journal of American Academy of Otolaryngology-Head and Neck Surgery. 2004; 130:157–163. [PubMed: 14990910]
3. Tsao GJ, Fijalkowski N, Most SP. Validation of a grading system for lateral nasal wall insufficiency. Allergy & rhinology. 2013; 4:e66–68. [PubMed: 24124639]
4. Zoumalan RA, Larrabee WF Jr, Murakami CS. Intraoperative suction-assisted evaluation of the nasal valve in rhinoplasty. Archives of facial plastic surgery. 2012; 14:34–38. [PubMed: 22250267]
5. Bhattacharyya N. Ambulatory sinus and nasal surgery in the United States: demographics and perioperative outcomes. The Laryngoscope. 2010; 120:635–638. [PubMed: 20058315]
6. Fattahi T. Internal nasal valve: significance in nasal air flow. Journal of oral and maxillofacial surgery : official journal of the American Association of Oral and Maxillofacial Surgeons. 2008; 66:1921–1926.
7. Murakami C. Nasal valve collapse. Ear, nose, & throat journal. 2004; 83:163–164.
8. Rhee JS, Weaver EM, Park SS, et al. Clinical consensus statement: Diagnosis and management of nasal valve compromise. Otolaryngology--head and neck surgery : official journal of American Academy of Otolaryngology-Head and Neck Surgery. 2010; 143:48–59. [PubMed: 20620619]

9. Elwany S, Thabet H. Obstruction of the nasal valve. The Journal of laryngology and otology. 1996; 110:221–224. [PubMed: 8730354]
10. Schlosser RJ, Park SS. Functional nasal surgery. Otolaryngologic clinics of North America. 1999; 32:37–51. [PubMed: 10196437]
11. Kasperbauer JL, Kern EB. Nasal valve physiology. Implications in nasal surgery. Otolaryngologic clinics of North America. 1987; 20:699–719. [PubMed: 3320865]
12. Teichgraeber JF, Wainwright DJ. The treatment of nasal valve obstruction. Plastic and reconstructive surgery. 1994; 93:1174–1182. discussion 1183-1174. [PubMed: 8171137]
13. Miman MC, Deliktas H, Ozturan O, Toplu Y, Akarcay M. Internal nasal valve: revisited with objective facts. Otolaryngology--head and neck surgery : official journal of American Academy of Otolaryngology-Head and Neck Surgery. 2006; 134:41–47. [PubMed: 16399179]
14. Grymer LF. Reduction rhinoplasty and nasal patency: change in the cross-sectional area of the nose evaluated by acoustic rhinometry. The Laryngoscope. 1995; 105:429–431. [PubMed: 7715390]
15. Hilberg O, Jackson AC, Swift DL, Pedersen OF. Acoustic rhinometry: evaluation of nasal cavity geometry by acoustic reflection. Journal of applied physiology. 1989; 66:295–303. [PubMed: 2917933]
16. Roithmann R, Cole P, Chapnik J, Shpirer I, Hoffstein V, Zamel N. Acoustic rhinometry in the evaluation of nasal obstruction. The Laryngoscope. 1995; 105:275–281. [PubMed: 7877416]
17. Bloom JD, Sridharan S, Hagiwara M, Babb JS, White WM, Constantinides M. Reformatted computed tomography to assess the internal nasal valve and association with physical examination. Archives of facial plastic surgery. 2012; 14:331–335. [PubMed: 22986939]
18. Moche JA, Cohen JC, Pearlman SJ. Axial computed tomography evaluation of the internal nasal valve correlates with clinical valve narrowing and patient complaint. International forum of allergy & rhinology. 2013; 3:592–597. [PubMed: 23255507]
19. Poetker DM, Rhee JS, Mocan BO, Michel MA. Computed tomography technique for evaluation of the nasal valve. Archives of facial plastic surgery. 2004; 6:240–243. [PubMed: 15262718]
20. Suh MW, Jin HR, Kim JH. Computed tomography versus nasal endoscopy for the measurement of the internal nasal valve angle in Asians. Acta oto-laryngologica. 2008; 128:675–679. [PubMed: 18568504]
21. Apaydin F. Nasal valve surgery. Facial plastic surgery : FPS. 2011; 27:179–191. [PubMed: 21404160]
22. Ishii LE, Rhee JS. Are diagnostic tests useful for nasal valve compromise? The Laryngoscope. 2013; 123:7–8. [PubMed: 23280938]
23. Englhard AS, Wiedmann M, Ledderose GJ, et al. Imaging of the internal nasal valve using long-range Fourier domain optical coherence tomography. The Laryngoscope. 2016; 126:E97–E102. [PubMed: 26599137]
24. Huang D, Swanson EA, Lin CP, et al. Optical coherence tomography. Science. 1991; 254:1178–1181. [PubMed: 1957169]
25. Armstrong J, Leigh M, Walton I, et al. In vivo size and shape measurement of the human upper airway using endoscopic longrange optical coherence tomography. Optics express. 2003; 11:1817–1826. [PubMed: 19466064]
26. Jing J, Zhang J, Loy AC, Wong BJ, Chen Z. High-speed upper-airway imaging using full-range optical coherence tomography. Journal of biomedical optics. 2012; 17:110507. [PubMed: 23214170]
27. Volgger V, Sharma GK, Jing JC, et al. Long-range Fourier domain optical coherence tomography of the pediatric subglottis. International journal of pediatric otorhinolaryngology. 2014
28. Ishii LE, Tollefson TT, Basura GJ, et al. Clinical Practice Guideline: Improving Nasal Form and Function after Rhinoplasty Executive Summary. Otolaryngology--head and neck surgery : official journal of American Academy of Otolaryngology-Head and Neck Surgery. 2017; 156:205–219. [PubMed: 28145848]
29. Barrett DM, Casanueva FJ, Cook TA. Management of the Nasal Valve. Facial plastic surgery clinics of North America. 2016; 24:219–234. [PubMed: 27400837]
30. Marotta JC, Becoats K. Intraoperative Endoscopic Suction-Assisted Evaluation of the Nasal Valve. JAMA facial plastic surgery. 2016; 18:171–176. [PubMed: 26769063]

31. Shaida AM, Kenyon GS. The nasal valves: changes in anatomy and physiology in normal subjects. Rhinology. 2000; 38:7–12. [PubMed: 10780041]
32. Grymer LF, Hilberg O, Pedersen OF, Rasmussen TR. Acoustic rhinometry: values from adults with subjective normal nasal patency. Rhinology. 1991; 29:35–47. [PubMed: 1710069]
33. Haight JS, Cole P. The site and function of the nasal valve. The Laryngoscope. 1983; 93:49–55. [PubMed: 6823174]
34. Jones AS, Wight RG, Stevens JC, Beckingham E. The nasal valve: a physiological and clinical study. The Journal of laryngology and otology. 1988; 102:1089–1094. [PubMed: 3225517]
35. Berry RB. Nasal resistance before and after rhinoplasty. British journal of plastic surgery. 1981; 34:105–111. [PubMed: 7459515]
36. Friedman M, Ibrahim H, Lee G, Joseph NJ. A simplified technique for airway correction at the nasal valve area. Otolaryngology--head and neck surgery : official journal of American Academy of Otolaryngology-Head and Neck Surgery. 2004; 131:519–524. [PubMed: 15467629]
37. Goode RL. Surgery of the incompetent nasal valve. The Laryngoscope. 1985; 95:546–555. [PubMed: 3887077]
38. Lazarow FB, Ahuja GS, Chin Loy A, et al. Intraoperative long range optical coherence tomography as a novel method of imaging the pediatric upper airway before and after adenotonsillectomy. International journal of pediatric otorhinolaryngology. 2015; 79:63–70. [PubMed: 25479699]

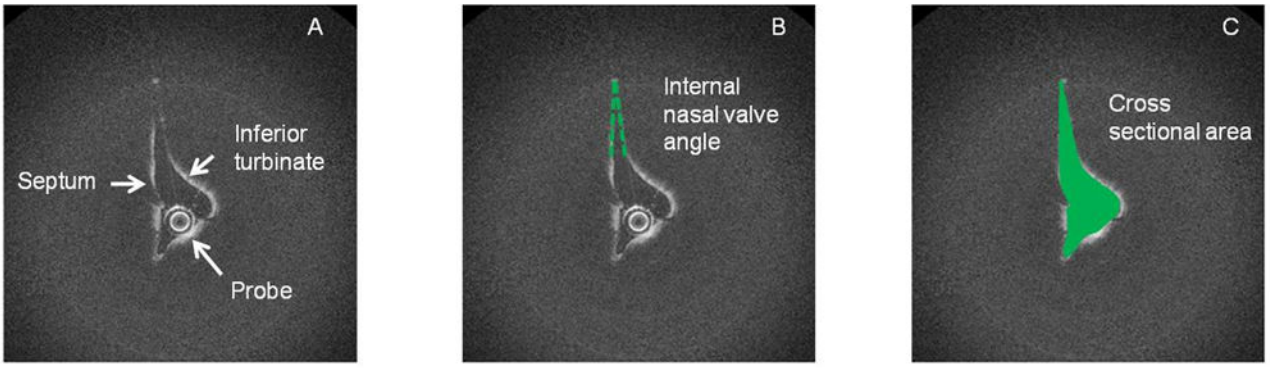

Figure 1.

Optical coherence tomography picture of a left internal nasal valve. (A) The internal nasal valve was identified by the anterior head of the inferior turbinate and the septum. (B) The angle of the internal nasal valve was measures between the septum and the lateral nasal wall. (C) The cross-sectional area was identified.

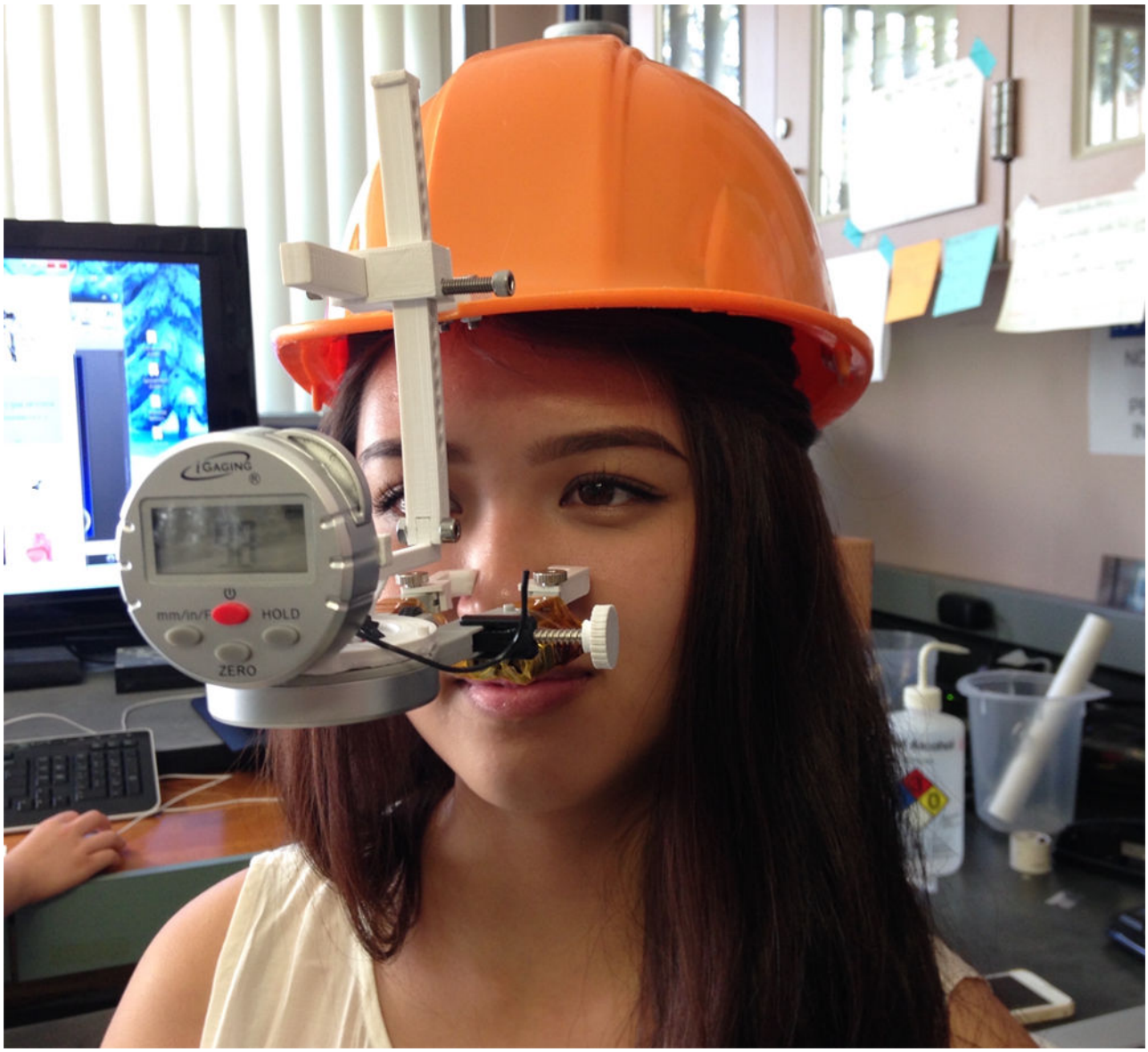

Figure 2.

Before starting OCT imaging, a specially designed nasal device was placed externally and unilaterally over the nasal valve area. The caliper has inward facing points to which a small blunt footpad is attached. A dial provides a measurement of displacement. The caliper is easily adjusted to either be in non-contact, near contact, or in contact with the lateral sidewall of the nose at the level of the upper lateral cartilage. Adjustment of the dial (digital readout) allows gentle displacement of the sidewall. Patients were asked to breathe normally while the displacement/applied pressure was slowly increased. OCT imaging was performed at the onset of subjective nasal obstruction. This procedure was repeated twice and the mean for both time points was calculated. The process was repeated on the opposite side.

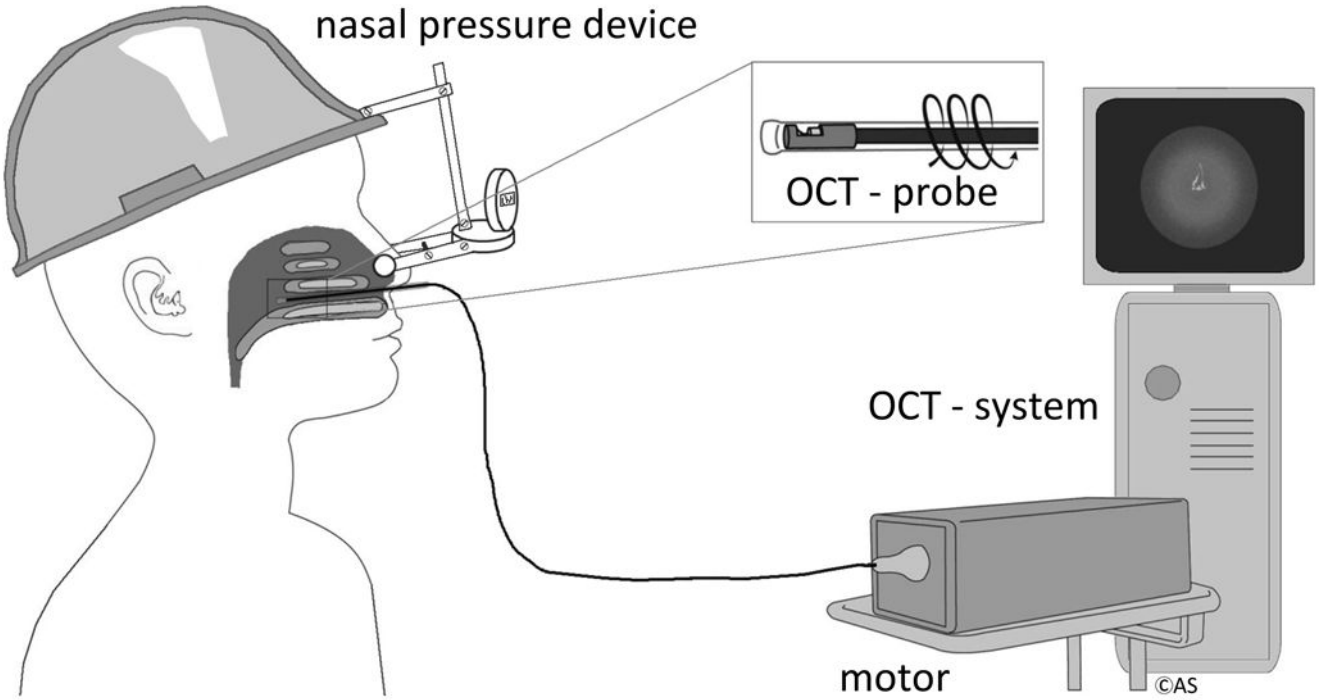

Figure 3.

OCT setup: OCT imaging was performed on awake, seated subjects. Probe rotation and pullback, data acquisition and real-time image display were controlled by Windows-based software. OCT probes were encased in a transparent, single-use and sterilized fluorinated ethylenepropylene sheath. For a part of the examinations a specially designed nasal device was placed externally and pressure was put unilaterally over the nasal valve area.

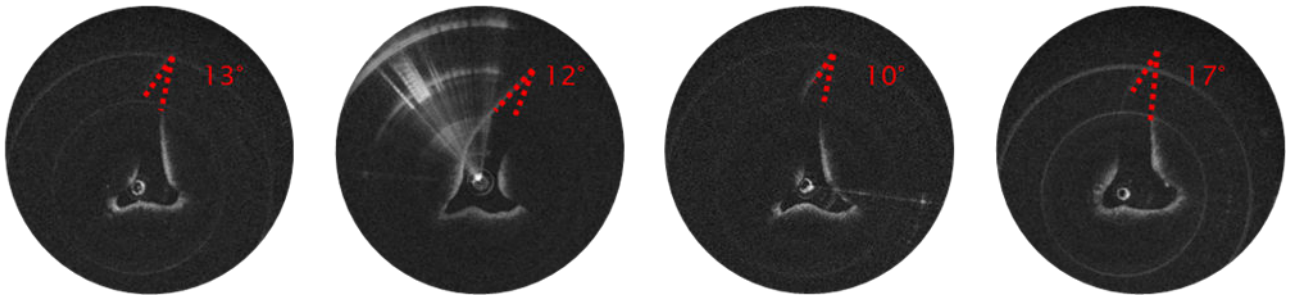

Figure 4.

OCT pictures of a right internal nasal valve (left: under normal conditions, second from left: during forced inspiration, second from right: with external pressure over the INV area, right after application of nasal decongestant)

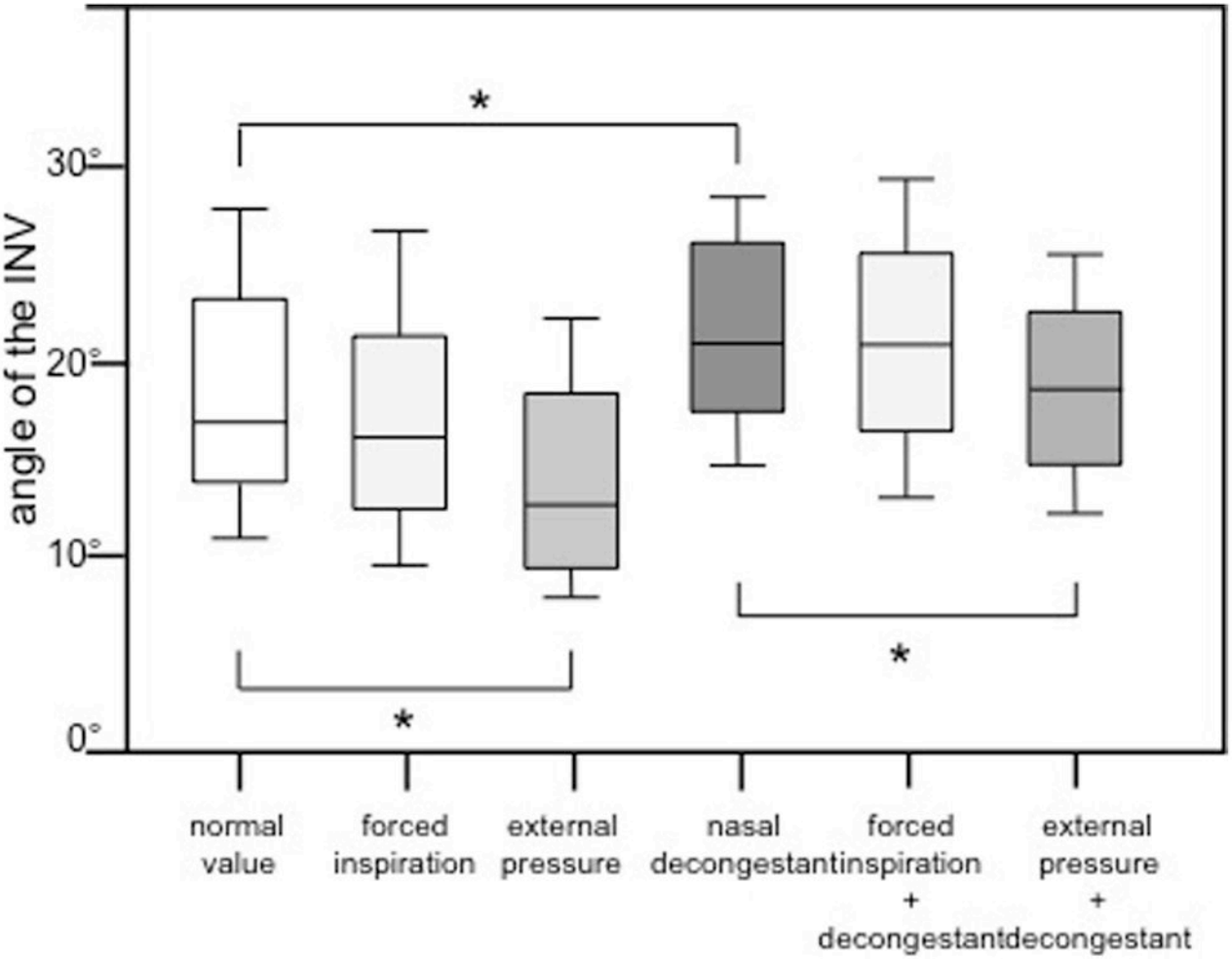

Figure 5.

Internal nasal valve angle measured by OCT in normal condition, during inspiration, with external pressure over the nasal valve area, after application of nasal decongestant, during inspiration after application of nasal decongestant and with external pressure over the nasal valve area after application of nasal decongestant. Group comparisons were done using the Kruskal-Wallis test followed by Dunn's test (*: $p < 0.05$).

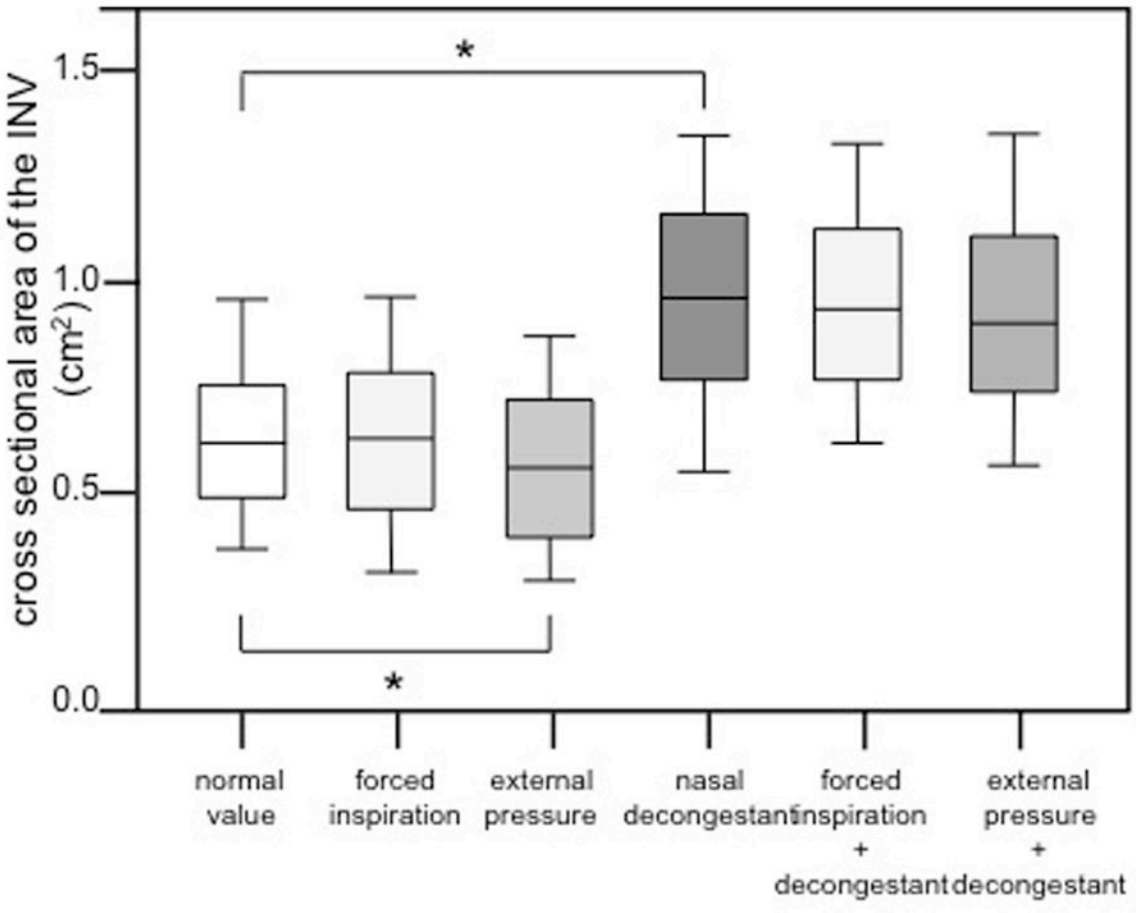

Figure 6.

Internal nasal valve cross sectional area measured by OCT in normal condition, during inspiration, with external pressure over the nasal valve area, after application of nasal decongestant, during inspiration after application of nasal decongestant and with external pressure over the nasal valve area after application of nasal decongestant. Group comparisons were done using the Kruskal-Wallis test followed by Dunn's test (*: $p < 0.05$).